

Following the Fermi level in the $\text{Bi}_2\text{Te}_{3-x}\text{Se}_x$ series through thermopower

Ana Akrap,^{1,*} Alberto Ubaldini,¹ Enrico Giannini,¹ and László Forró²

¹*University of Geneva, CH-1211 Geneva 4, Switzerland*

²*EPFL, Lausanne, Switzerland*

(Dated: October 16, 2012)

We report a detailed study of the temperature and composition dependence of the resistivity and thermopower for a series of bismuth chalcogenides $\text{Bi}_2\text{Te}_{3-x}\text{Se}_x$. The temperature dependence of the thermopower can be semi-quantitatively described by a simple model for an extrinsic semiconductor. We show that, by substituting selenium for tellurium, the Fermi level can be continuously tuned from the valence band into the conduction band. The maximum values of the thermopower, bulk band gap as well the activation energy are found for $x \approx 1$.

PACS numbers: 72.20.Pa, 72.20.-i, 72.80.-r

Layered bismuth chalcogenides $\text{Bi}_2\text{Te}_{3-x}\text{Se}_x$ are a family of narrow-band semiconductors, well known since the 1950's for their exceptional thermoelectric properties.¹ Bi_2Te_3 has the highest known thermoelectric figure of merit zT at room temperature, and is widely used in room-temperature thermoelectric applications.

Recently, bismuth chalcogenides were rediscovered within the novel context of topological insulators. They were among the first identified three-dimensional topological insulators.^{2,3} The surface states in $\text{Bi}_2\text{Te}_{3-x}\text{Se}_x$ are simple since only one Dirac cone crosses the band gap.^{4,5} However, in spite of a relatively large band gap (200 – 300 meV), bulk conductivity of known bismuth chalcogenides is too high and hinders the observation of topological surface states, even in the most compensated compound $\text{Bi}_2\text{Te}_2\text{Se}$.^{6,7} Throughout this series, the Fermi level is found either within the conduction or valence band.

In this paper we study the detailed thermoelectric properties of bismuth chalcogenides to clarify the relation between the composition and position of the Fermi level. We investigate ten different compositions of the $\text{Bi}_2\text{Te}_{3-x}\text{Se}_x$ series, where Se content is tuned from $x = 0$ to 3. We find that thermopower $S(T)$ may be semi-quantitatively explained by the standard extrinsic semiconductor model.¹ Most importantly, thermopower shows that tuning Te/Se content leads to a steady shift of chemical potential, from the valence band in the p-type Bi_2Te_3 , to the conduction band in the n-type Bi_2Se_3 . The highest value of the thermopower is found at $x = 1$ and it corresponds to the lowest Fermi temperature.

Single crystals of $\text{Bi}_2\text{Te}_{3-x}\text{Se}_x$ were grown by the floating zone method from the stoichiometric ratio of metallic bismuth and chalcogenide elements.⁸ The unit cell of a $\text{Bi}_2\text{Te}_{3-x}\text{Se}_x$ compound consists of quintuple Te/Se–Bi–Te/Se–Bi–Te/Se layers stacked along the c -axis direction.^{9,10} The quintuple layers are bound by weak van der Waals interaction. For most compositions, crystals readily cleave and expose shiny surfaces. We investigated ten different compositions, given by the Se content $x = 0, 0.6, 0.9, 0.95, 1, 1.3, 1.5, 2$ and 3. The resistivity and thermopower were measured simultaneously using a custom setup. Crystals were cleaved and cut

into thin bars of approximately $1.5 \times 0.5 \times 0.02$ mm³. The resistivity was measured using a standard four-probe technique. Thermopower was determined using a dc method. The sample was fixed to a ceramic surface with a small heater attached next to it, and the thermal gradient was determined using a chromel-constantan differential thermocouple. The bulk band gap was determined through transmission and reflection measurements on cleaved thin flakes, using a Bruker Hyperion microscope.⁸

The behavior of the resistivity throughout the series is shown in Fig. 1(a) at room temperature and at 10 K. A pronounced maximum in ρ occurs around $x = 0.9$. A more detailed temperature dependence of the resistivity is shown in Fig. 1(b) in an Arrhenius plot, for several different compositions x . While most samples exhibit a weakly metallic resistivity, we observe an activated behavior for $x = 0.9, 0.95, 1$ and 1.3. This is precisely in the x range where $\rho(x)$ has maximum value. However, the activation energies are small and range from ~ 4.5 meV for $x = 0.95, 1$ and 1.3, to ~ 40 meV for $x = 0.9$.

The stoichiometry dependence of the bulk band gap is shown in Fig. 1(c). It was determined through the optical reflection and transmission measurements by following the energy of the onset of the Fabry-Perot interferences, similar to the previous high pressure studies of bismuth chalcogenides.^{7,11,12} The details of the measurement will be published elsewhere.⁸ The bulk band gap spans from approximately 200 meV in Bi_2Te_3 to 300 meV in Bi_2Se_3 , and reaches a maximum of 325 meV in $\text{Bi}_2\text{Te}_{2.1}\text{Se}_{0.9}$. It is interesting to note that the maximum band gap happens for the same stoichiometry ($x \approx 1$) for which resistivity is maximum. While the band gap is determined by the band structure, the transport gap is linked to the defects which lead to impurity doping. Recent theoretical work by Skinner *et al.* shows there is a relation between these two quantities, and the activation energy of the resistivity in a compensated topological insulator is proportional to the band gap.¹³

The dc transport activation energy never exceeded 40 meV, which points to the fact that $\text{Bi}_2\text{Te}_{3-x}\text{Se}_x$ compounds are always doped by impurities. The impurity levels are particularly evident at low temperatures,

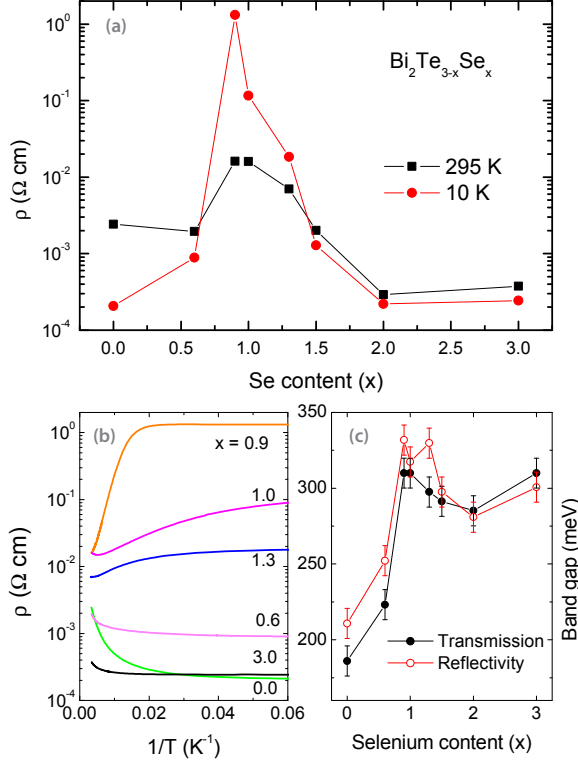


FIG. 1. (Color online) (a) Resistivity at high and low temperature for varying composition, from Bi_2Te_3 to Bi_2Se_3 . A maximum ρ occurs close to $\text{Bi}_2\text{Te}_2\text{Se}$. (b) Temperature dependence of resistivity for several different compositions (Selenium stoichiometries), x . (c) Bulk band gap is shown for the whole series.

where $\rho(T)$ shows very little temperature dependence (Fig. 1(b)). Small activation energies accompanied by an almost constant ρ at low temperatures suggest that the donor or acceptor levels within the bulk gap are important contributors to the conduction. Impurity levels broaden into a band which overlaps with the valence or conduction band. This impurity band probably lies at the edge of the conduction or valence band.¹⁴

There are several reasons why impurity doping inevitably occurs in this series. Bismuth and tellurium have a similar Pauling electronegativity.¹⁵ Bismuth atoms therefore occupy tellurium sites and make for a high concentration of negatively charged defects, which is why Bi_2Te_3 crystals are most often p -type.¹⁶ Selenium, on the other hand, has a high fugacity, and the accumulation of selenium vacancies causes the n -type behavior of Bi_2Se_3 .¹⁷ For the intermediate stoichiometries, both of the above types of disorder, vacancies, and antisite defects, are present and lead to intrinsic doping. In reality, when the composition of the compound is tuned from $\text{Bi}_2\text{Te}_{3+\delta}$ to $\text{Bi}_2\text{Se}_{3-\delta}$, one passes from a system with ex-

cess Te, towards a Se-deficient compound. Around the composition $x = 1$, the Se/Te sublattice is expected to be ordered which significantly reduces the number of defects in the structure, decreasing conductivity.

A very reliable method to follow the progression from p to n -type conductor is by measuring thermopower. This is particularly simple in a situation where there is only one relevant electronic band. Fig. 2(a) shows the dependence of thermopower on Se content, x , at several different temperatures. There is a very sharp sign change taking place between $x = 0.95$ and $x = 1.0$. For $x \geq 1$ the thermopower becomes negative, meaning that there is a transition from p -type to n -type conduction. This transition is illustrated within inset of Fig. 2(a) cartoon.

For thermoelectric applications, it is important to optimize the figure of merit zT . In applications that do not require maintaining a temperature gradient, the power factor S^2/ρ should be maximized. The power factor ranges between 10 to 50 $\mu\text{W}/(\text{K}^2\text{cm})$ for the series of the samples we study here. These values are similar to those of Sokolov *et al*, and display a similar doping dependence.¹⁸ Maximum power factor of 50 $\mu\text{W}/(\text{K}^2\text{cm})$ takes place for $x = 2$, and minimum 10 $\mu\text{W}/(\text{K}^2\text{cm})$ occurs for $x = 1$ where both the thermopower and the resistivity are maximum.

Fig. 2(b) shows a detailed temperature dependence of thermopower $S(T)$ for nine different compositions x . All of the samples are either n or p type. The only exception is the $x = 0.9$ sample, which is p -type at high temperatures, and n -type below ~ 50 K. Leaving the $x = 0.9$ composition aside, let us focus on the temperature dependence of thermopower in the other nine compounds.

The thermopower of a heavily-doped semiconductor on the metallic side of the metal-insulator transition is given by:¹

$$S = \pm \frac{k_B}{e} \left[\eta_F - \frac{(r + 5/2)F_{r+3/2}(\eta_F)}{(r + 3/2)F_{r+1/2}(\eta_F)} \right] \quad (1)$$

Here $\eta_F = E_F/(k_B T)$ is the reduced Fermi energy; the parameter r describes the energy dependence of the scattering time, and

$$F_n = \int_0^\infty d\eta \frac{\eta^n}{1 + \exp(\eta - \eta_F)} \quad (2)$$

is the Fermi integral. E_F is measured from the bottom of the conduction band for the n -type, or the top of the valence band in the case of a p -type semiconductor. To describe the energy dependence of the scattering time parameter, we take the standard value¹ $r = -0.5$ for acoustic phonon scattering and calculate $S(T)$ assuming a set of temperature-independent values for E_F . A more correct method would be to determine E_F from the charge balance constraint,¹⁹ but since the charge doping comes from unintentional impurities, a precise amount of carriers is unknown.

For Bi_2Se_3 , the carrier density n may be estimated by comparing the resistivity data in Fig. 1 to the results

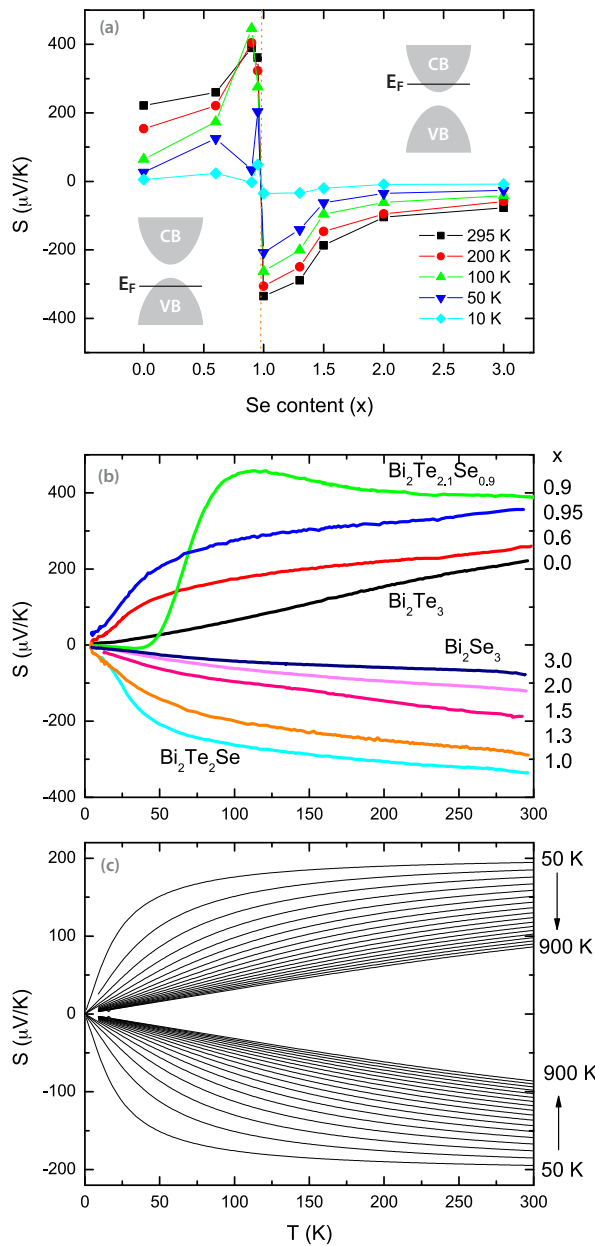


FIG. 2. (Color online) The dependence of thermopower on Selenium stoichiometry is shown in (a), at five different temperatures. (b) The experimental temperature dependence for nine different stoichiometries (given by Selenium content x). (c) Results of a simple model calculation given by Eq. 2. The Fermi level is varied between 50 K and 900 K in steps of 50 K (from 4.3 to 77.6 meV). Note the different scales in (b) and (c).

reported by Butch *et al.*²⁰, which gives a result of $n \sim 10^{18} - 10^{19} \text{ cm}^{-3}$.

Results for the calculated temperature dependence of thermopower are shown in Fig. 2(c) for E_F/k_B , ranging from 50 K to 900 K (corresponding to the E_F between

4.3 and 77.6 meV), in steps of 50 K. This ballpark for E_F seems to be in fair agreement with ARPES results from some members of the series. For example, Hor *et al.*²¹ observed a Fermi level of 50 meV in Bi_2Se_3 and Chen *et al.*²² saw $E_F \approx 45$ meV in Bi_2Te_3 .

The measurements of quantum oscillations for Bi_2Se_3 show that the fundamental state of the system is metallic and that carrier density can be tuned by several orders of magnitude via controlling the stoichiometry.²³ When changing the carrier density from 10^{17} to 10^{18} cm^{-3} , the Fermi temperature moves from 80 K to 1100 K. This is in good agreement with the approximate value of 900 K suggested for our Bi_2Se_3 sample by the calculated series in Fig. 2(c).

The simple semiconductor model given by the Eq. 2 captures our experimental results quite well. The higher values of E_F lead to a thermopower almost linear in temperature, very similar to the one measured in Bi_2Te_3 and Bi_2Se_3 . A smaller E_F leads to a thermopower with a distinct change in slope for $k_B T < E_F$. Such a shape of $S(T)$ is similar to what we measure for $x \approx 1$. However, the calculated values of S are smaller than the measured thermopower. This may be due to additional contributions to the thermopower not taken into account by the model, such as the phonon drag, or because the parameter r is not simply -0.5 , but has a temperature and composition dependence.^{24,25}

In the calculated $S(T)$ curves, the temperature slope changes at temperatures $T \sim E_F/k_B$. With this in mind, one might conclude from Fig. 2(b) that samples with $x = 0.6, 0.9$, and 1.0 all have $E_F \sim 4$ meV. On the contrary, Fermi levels in pure Bi_2Te_3 and Bi_2Se_3 should be above room temperature since no clear change in slope is visible from our thermopower data.

For $x = 0.9$ ($\text{Bi}_2\text{Te}_{2.1}\text{Se}_{0.9}$), $S(T)$ seems to be an exception. The temperature dependence is different than in the rest of the series. S rises above $400 \mu\text{V/K}$ at 100 K, and then precipitously drops below 100 K. This is the only composition for which the sample is p -type at high temperatures and n -type at low temperatures, suggesting that the charge carriers exist in more than one band. This sample also has the highest resistivity within the series, as shown in Fig. 1(b), and among the highest bulk band gaps (~ 325 meV). This more complex behavior may possibly be linked to additional impurity bands.

To summarize, we have presented a systematic study of the composition and temperature dependence of thermopower within the bismuth chalcogenide $\text{Bi}_2\text{Te}_{3-x}\text{Se}_x$ series. The maximum resistivity, thermopower, and bulk band gap occur with compositions where $x \approx 1$. For this composition, the Te/Se sublattice is maximally ordered, which reduces the defects in the crystal lattice and diminishes impurity doping.⁶

The value of thermopower at a given temperature can be tuned by changing the stoichiometry. Starting from the p -type Bi_2Te_3 , upon replacing a part of Te atoms with Se, thermopower is strongly enhanced, and with the composition $\text{Bi}_2\text{Te}_2\text{Se}$ thermopower changes its sign. As

the amount of Se is increased, the value of thermopower decreases. The temperature dependence of thermopower may be semi-quantitatively described by a simple model for an extrinsic semiconductor. Here, the Fermi level E_F decreases from Bi_2Te_3 towards $\text{Bi}_2\text{Te}_{2.05}\text{Se}_{0.95}$, reaching a minimum of approximately 4 meV. When more Se is replaced for Te, the Fermi level E_F starts increasing again.

Both the bulk band gap and the Fermi level can be tuned by controlling Se/Te stoichiometry.

We would like to thank Kamran Behnia, Brian C. Sales and Nathaniel Miller for helpful advice and comments. Research was supported by the Swiss NSF through grant No. 200020-135085 and its NCCR MaNEP. A.A. acknowledges funding from “Boursières d’Excellence” of the University of Geneva.

-
- * ana.akrap@unige.ch
- ¹ H. Goldsmid, *Thermoelectric Refrigeration* (Temple Press Books Ltd, London, 1964).
 - ² H. Zhang, C.-X. Liu, X.-L. Qi, X. Dai, Z. Fang, and S.-C. Zhang, *Nature Phys.* **5**, 438 (2009).
 - ³ L.-L. Wang and D. D. Johnson, *Phys. Rev. B* **83**, 241309 (2011).
 - ⁴ M. Hasan, H. Lin, and A. Bansil, *Physics* **2**, 108 (2009).
 - ⁵ T. Valla, Z.-H. Pan, D. Gardner, Y. S. Lee, and S. Chu, *Phys. Rev. Lett.* **108**, 117601 (2012).
 - ⁶ Z. Ren, A. A. Taskin, S. Sasaki, K. Segawa, and Y. Ando, *Phys. Rev. B* **82**, 241306(R) (2010).
 - ⁷ A. Akrap, M. Tran, A. Ubaldini, J. Teyssier, E. Gianini, D. van der Marel, P. Lerch, and C. C. Homes, arXiv:1209.3593 (2012).
 - ⁸ A. Ubaldini, To be submitted.
 - ⁹ S. Nakajima, *Journal of Physics and Chemistry of Solids* **24**, 479 (1963).
 - ¹⁰ P. Bayliss, *Amer. Mineral.* **76**, 257 (1991).
 - ¹¹ R. Vilaplana, O. Gomis, F. J. Manjón, A. Segura, E. Pérez-González, P. Rodríguez-Hernández, A. Muñoz, J. González, V. Marín-Borrás, V. Muñoz Sanjosé, C. Drasar, and V. Kucek, *Phys. Rev. B* **84**, 104112 (2011).
 - ¹² Segura, A. and Panchal, V. and Sánchez-Royo, J. F. and Marín-Borrás, V. and Muñoz-Sanjosé, V. and Rodríguez-Hernández, P. and Muñoz, A. and Pérez-González, E. and Manjón, F. J. and González, J., *Phys. Rev. B* **85**, 195139 (2012).
 - ¹³ B. Skinner, T. Chen, and B. Shklovskii, arXiv:1208.4601v2 (2012).
 - ¹⁴ H. J. Goldsmid, *Journal of Electronic Materials*, **41**, 2126 (2012).
 - ¹⁵ E. Gaudin, S. Jobic, M. Evain, and R. Brec, *Materials Research Bulletin* **30**, 549 (1995).
 - ¹⁶ V. Kul’bachinskii, A. Kaminskii, K. Kindo, Y. Narumi, K. Suga, P. Lostak, and P. Svanda, *JETP Letters* **73**, 352 (2001-04-18).
 - ¹⁷ T. Plecháček, J. Navrátil, and J. Horák, *Journal of Solid State Chemistry* **165**, 35 (2002).
 - ¹⁸ O. Sokolov, S. Skipidarov, N. Duvankov, and G. Shabunina, *Inorganic Materials* **43**, 8 (2007-01-01).
 - ¹⁹ B. C. Sales, M. A. McGuire, A. S. Sefat, and D. Mandrus, *Physica C: Superconductivity* **470**, 304 (2010).
 - ²⁰ N. P. Butch, K. Kirshenbaum, P. Syers, A. B. Sushkov, G. S. Jenkins, H. D. Drew, and J. Paglione, *Physical Review B* **81**, 241301 (2010).
 - ²¹ Y. S. Hor, A. Richardella, P. Roushan, Y. Xia, J. G. Checkelsky, A. Yazdani, M. Z. Hasan, N. P. Ong, and R. J. Cava, *Physical Review B* **79**, 195208 (2009).
 - ²² Y. L. Chen, J. G. Analytis, J. H. Chu, Z. K. Liu, S. K. Mo, X. L. Qi, H. J. Zhang, D. H. Lu, X. Dai, Z. Fang, S. C. Zhang, I. R. Fisher, Z. Hussain, and Z. X. Shen, *Science* **325**, 178 (2009).
 - ²³ B. Fauqué, N. Butch, P. Syers, J. Paglione, S. Wiedmann, A. Collaudin, B. Grena, U. Zeitler, and K. Behnia, arXiv:1209.1312.
 - ²⁴ V. A. Kulbachinskii, V. G. Kytin, A. A. Kudryashov, and P. M. Tarasov, *Solid State Chemistry and Materials Science of Thermoelectric Materials*, *Journal of Solid State Chemistry* **193**, 47 (2012).
 - ²⁵ V. A. Kulbachinskii, H. Negishi, M. Sasaki, Y. Giman, M. Inoue, P. Losták, and J. Horák, *Physica Status Solidi (b)* **199**, 505 (1997).